VOL. 202, NO. 2 THE AMERICAN NATURALIST AUGUST 2023

Disentangling Mechanical and Sensory Modules in the Radiation of Noctilionoid Bats

Gregory L. Mutumi,[1,*] Ronald P. Hall,[2] Brandon P. Hedrick,[3] Laurel R. Yohe,[4,5] Alexa Sadier,[6] Kalina T. J. Davies,[7] Stephen J. Rossiter,[7] Karen E. Sears,[6] Liliana M. Dávalos,[5,8] and Elizabeth R. Dumont[1]

1. Life and Environmental Sciences, University of California, Merced, California 95343; 2. Graduate Program in Quantitative Systems Biology, University of California, Merced, California 95343; 3. Department of Biomedical Sciences, College of Veterinary Medicine, Cornell University, Ithaca, New York 14853; 4. Department of Earth and Planetary Science, Yale University, New Haven, Connecticut 06521; 5. Department of Ecology and Evolution, Stony Brook University, Stony Brook, New York 11790; 6. Department of Ecology and Evolutionary Biology, University of California, Los Angeles, California 90095; 7. School of Biological and Behavioural Sciences, Queen Mary University of London, London, United Kingdom; 8. Consortium for Inter-Disciplinary Environmental Research, School of Marine and Atmospheric Sciences, Stony Brook University, Stony Brook, New York 11794

Submitted March 6, 2021; Accepted January 25, 2023; Electronically published June 12, 2023

Online enhancements: supplemental PDF, videos, Excel table, sample CT scans.

ABSTRACT: With diverse mechanical and sensory functions, the vertebrate cranium is a complex anatomical structure whose shifts between modularity and integration, especially in mechanical function, have been implicated in adaptive diversification. Yet how mechanical and sensory systems and their functions coevolve, as well as how their interrelationship contributes to phenotypic disparity, remain largely unexplored. To examine the modularity, integration, and evolutionary rates of sensory and mechanical structures within the head, we analyzed hard and soft tissue scans from ecologically diverse bats in the superfamily Noctilionoidea, a clade that ranges from insectivores and carnivores to frugivores and nectarivores. We identified eight regions that evolved in a coordinated fashion, thus recognizable as evolutionary modules: five associated with bite force and three linked to olfactory, visual, and auditory systems. Interrelationships among these modules differ between Neotropical leaf-nosed bats (family Phyllostomidae) and other noctilionoids. Consistent with the hypothesis that dietary transitions begin with changes in the capacity to detect novel food items followed by adaptations to process them, peak rates of sensory module evolution predate those of some mechanical modules. We propose that the coevolution of structures influencing bite force, olfaction, vision, and hearing constituted a structural opportunity that allowed the phyllostomid ancestor to take advantage of existing ecological opportunities and contributed to the clade's remarkable radiation.

Keywords: cranium, integration, modularity, sensory, mechanical, trait relationships.

Introduction

How multiple traits are organized and reorganized, as well as how that organization impacts the nature of evolutionary change, are outstanding questions in biology (Esteve-altava 2017). Among vertebrates, the morphology of the cranium is compartmentalized into numerous semiautonomous modules that display strong internal correlation relative to their correlation with other modules, with some of these correlations conserved across mammals (Atchley and Hall 1991; Goswami 2006; Porto et al. 2009; Goswami and Polly 2010; Assis et al. 2016; Goswami and Finarelli 2016; Evans et al. 2017; Felice and Goswami 2017; Bardua et al. 2019). The impact of modularity on the nature of morphological evolution is the subject of ongoing inquiry. Some studies have linked higher evolvability and increased phenotypic diversity to the boundaries prescribed by highly integrated modules (Esteve-altava 2017; Felice et al. 2018; Hedrick et al. 2020), while others have found that modularity influences the direction of evolutionary change but not its rate (Goswami et al. 2014; Conith et al. 2019; Rossoni et al. 2019; Watanabe et al. 2019). Despite the importance

---

* Corresponding author; email: gmutumi@gmail.com.

ORCIDs: Mutumi, https://orcid.org/0000-0003-1911-2232; Hall, https://orcid.org/0000-0003-3467-361X; Hedrick, https://orcid.org/0000-0003-4446-3405; Yohe, https://orcid.org/0000-0003-1567-8749; Sadier, https://orcid.org/0000-0002-9907-3714; Davies, https://orcid.org/0000-0002-4258-4775; Rossiter, https://orcid.org/0000-0002-3881-4515; Sears, https://orcid.org/0000-0001-9744-9602; Dávalos, https://orcid.org/0000-0002-4327-7697; Dumont, https://orcid.org/0000-0002-7809-388X.

of sensory information for organismal function and the obvious physical and functional links between sensory and mechanical systems in the vertebrate skull, the modularity of cranial sensory systems and their relationship to mechanical modules has not been explicitly investigated.

Modularity results from processes acting at several biological scales (Cumming et al. 2006), from genotype to phenotype through development (Wagner et al. 2007; Klingenberg 2010; Felice et al. 2018; Zelditch and Goswami 2021). Although developmental gene regulatory networks are known to sometimes constrain or favor phenotypic evolution (Erwin and Davidson 2009; Davidson 2010; Mallarino et al. 2011), trait covariation within or between species may not reflect such underlying developmental modules (Conith et al. 2021). Instead, these evolutionary modules offer a composite, the product of complex interactions during ontogeny as well as over evolutionary time (Zelditch and Goswami 2021). Evolutionary modules may correspond to functional modules when they are associated with ecological functions, such as mammalian vertebrae (Jones et al. 2018) and flatfish crania (Evans et al. 2021). Evaluating trait integration among species involves assessing the strength and pattern of correlation within and between hypothesized functional modules. Beyond the idea that functional modules can be objects of selection, comparative analyses of functional modules can also point to the tempo of change across modules (Watanabe et al. 2019), corresponding to changing functions over time.

The diversity of cranial phenotypes associated with feeding within noctilionoid bats (superfamily Noctilionoidea) makes them an ideal system in which to investigate the relationships between mechanical and sensory modules through time. Neotropical noctilionoid bats include 248 species, 218 of which comprise the family Phyllostomidae (Fleming et al. 2020), commonly known as the Neotropical leaf-nosed bats. Most noctilionoid families are primarily insectivorous, and divergence among lineages presents as subtle variation in body size, foraging style, and echolocation calls (Freeman 2000; Rolfe 2011; Baker et al. 2012; Thiagavel et al. 2018; Rodriguez-Durán and Rosa 2020). Although phyllostomids maintain the ancestral multiharmonic echolocation calls, they have escaped strict insectivory and diversified into dietary niches that include nectar, fruit, vertebrates, and blood (fig. 1; also see fig. 1 in Dumont et al. 2012). This ecological diversity is reflected in the differential reliance of phyllostomid bats on a constellation of sensory and mechanical functions (Arbour et al. 2019; Fleming et al. 2020).

In this study, we test three broad hypotheses about functionally defined mechanical and sensory modules and their potential influence on ecomorphological diversity across Neotropical noctilionoid bats. First, we hypothesize that mechanical and sensory structures are independent suites of modules. Second, we hypothesize that mechanical and sensory modules have evolved at different rates. Third, we hypothesize that within each module the relationship between phenotypic disparity and rate of phenotypic evolution differs significantly from a null model in a manner consistent with either evolutionary facilitation or constraint (Felice et al. 2018). Given the fundamental link between cranial shape and bite force in phyllostomids (Dumont et al. 2014), we expect mechanical modules to exhibit higher than expected disparity relative to rates of evolution (Hu et al. 2016; Arlegi et al. 2018; Hedrick et al. 2020). We expect that sensory modules are more conserved than mechanical modules because while sensory modules do exhibit phenotypic variation (Hall et al. 2021), ecological diversification has likely resulted in less extensive reorganization of sensory structures. To gain a more nuanced understanding of their associations, we also explore the relationship between mechanical and sensory modules in clades, among lineages, and with respect to the evolution of module shapes.

Methods

Taxonomic Sample and 3D Imaging

We sampled 42 individuals from 35 species, covering all Neotropical families within Noctilionoidea (Phyllostomidae, Noctilionidae, Mormoopidae, Furipteridae, and Thyropteridae) and encompassing a broad range of dietary niches within the clade (fig. 1; table S1). All analyses incorporated the time-calibrated phylogeny of Rojas et al. (2016), pruned to reflect our sample (fig. 1). We repeated analyses with three different datasets: the complete dataset representing all noctilionoids; phyllostomids alone (34 individuals, 28 species), where dietary diversity is concentrated; and other nonphyllostomid noctilionoids combined (four families, eight individuals, seven species), all of which are insectivorous.

To quantify the sizes and shapes of all mechanical modules and two of the three sensory modules (the olfactory bulb and cochlea), we visualized the heads of bats using standard computed tomography (CT) for hard tissues. Bat specimens were scanned using a Nikon Metrology (X-Tek) HMXST225 micro-CT system at the Center for Nanoscale Systems at Harvard University. Three-dimensional images were processed following Hedrick et al. (2020). We generated image stacks using proprietary software associated with the X-Tek scanner (CTPro, Nikon Metrology, Tokyo), segmented image stacks using Mimics 16.0 (Materialise, Leuven, Belgium), created meshes using VGStudio Max 3.0 (Volume Graphics, Heidelberg), and exported them as PLY files. Three-dimensional landmarks were placed on these structures to quantify module shapes.

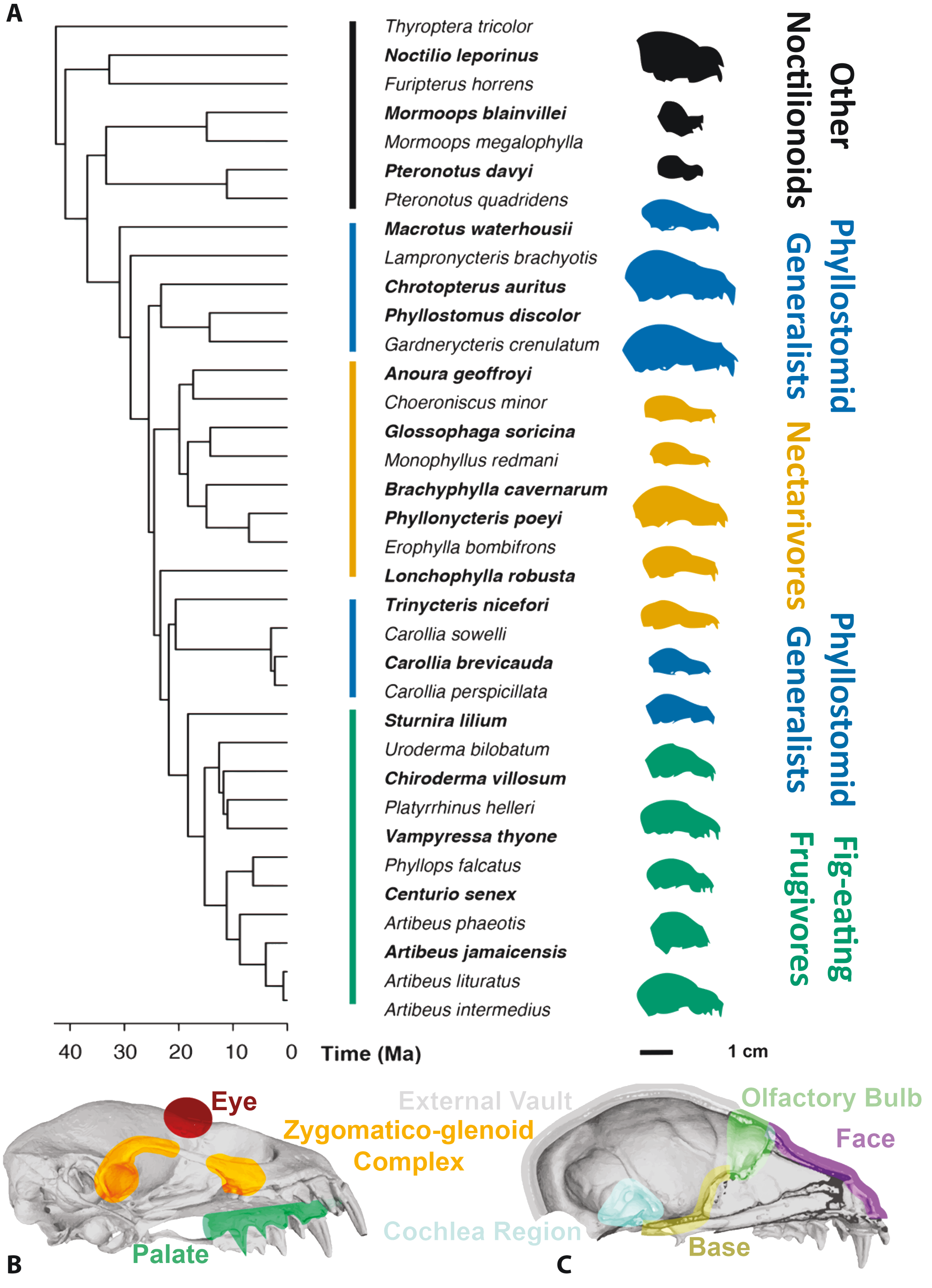

Figure 1: *A*, Tree of sampled taxa color coded by feeding guild. Silhouettes appear in the same sequence as the species in boldface type. The phylogeny is based on Rojas et al. (2016). Locations of sensory and mechanical modules are illustrated on a ventrolateral view of the external surface of the cranium (*B*) and a cutaway view illustrating the sagittal plane of the cranium (*C*).

For the eye, the third sensory structure, we used soft-tissue reconstructions of the orbital space published by Hall et al. (2021) based on diffusible iodine–based contrast-enhanced CT (Gignac et al. 2016) of the same specimens (Hedrick and Dumont 2018; table S1). We defined the orbital space surrounding the left eye by its muscular boundaries and eyelid and used the volume and centroid of the orbital space to create orbital spheres to serve as proxies for eye location and volume.

Placing Landmarks

Our dataset included a total of 322 landmarks: 43 fixed landmarks, 160 sliding semilandmarks on curves, 55 surface landmarks on the eye, and 64 surface landmarks on a patch placed on the palate (table S2 ; videos S1, S2) that were placed on 3D meshes using IDAV Landmark (ver. 3.6; Wiley et al. 2005). Sliding semi- and surface landmarks are adjusted to reduce their weight in the analysis and the effect of spacing on shape variation (Bookstein 1997; Gunz and Mitteroecker 2013). We placed external landmarks on the external surface of the cranium as per Hedrick et al. (2020). To landmark structures on internal surfaces of the bony skull, 3D models were digitally dissected in Geomagic Studio 2014 (3DSystems, Rock Hill, SC) to reveal the cochlea, the impression left by the olfactory bulb (anterior cranial fossa), and the internal surface of the cranial base.

For the eye, we placed 55 landmarks on the orbital spheres. Reducing the eye landmarks to seven (one in the center and six across perpendicular poles) did not change the results of tests for modularity (table S3), so we included all 55 eye landmarks in our analyses. Because our eye data are based on idealized and identical shapes, the results of our analyses reflect variation in the position and overall size of the eye. Throughout the landmarking process, we kept all parts of each specimen in the same coordinate system so that landmarks could be concatenated into a single file using custom R code. Sensitivity analysis confirmed that landmark density did not affect subsequent analyses of modularity hypotheses (table S4) or module integration (table S5). To employ phylogenetic comparative methods and adjust for unequal sample sizes in our analyses, we used species means for taxa represented by multiple individuals (seven species; table S1).

Defining Modules

To test hypotheses about modularity of sensory and mechanical systems, we grouped landmarks into eight hypothetical modules that encompass anatomical structures associated with specific functions (fig. 1; videos S1, S2). In this article, raw module "shape" is defined by its Procrustes coordinates in 3D space. We use covariance matrices of Procrustes coordinates to test hypotheses of modularity. Principal components (PCs) explaining 95% of the variation among Procrustes coordinates represent shape changes in our analyses of rates of module change across lineages through time. Finally, we use the first two PCs explaining variation among Procrustes coordinates as proxies of shape change to illustrate rates of shape evolution and changes in shape within individual modules over the phylogeny.

We hypothesized eight functional modules. We did not adjust the modules for allometry because the size of sensory structures is often directly related to function. Many studies have demonstrated clear links between cranial shape and variation in mechanical function (e.g., Dumont 2004; Dumont et al. 2009, 2012; Santana et al. 2012; Neaux et al. 2021). Here, we make inferences based on those linkages but do not directly measure mechanical variables. The shapes of sensory structures (e.g., olfactory bulb, cochlear region, and eye) are unlikely to perfectly reflect sensory ability. It is also likely that some shape variation in mechanical structures do not reflect functional variation (Gould and Lewontin 1979). Nevertheless, we propose that there is at least circumstantial evidence to suggest that each of our eight modules carries some functional signal.

We defined three sensory modules that encompass the olfactory bulb (smell), the cochlea (hearing), and the eye (vision; fig. 1; videos S1, S2). Enlarged eyes are associated with increased visual acuity (Müller and Peichl 2005; Müller et al. 2007; Land and Nilsson 2012; Eklöf et al. 2014; Veilleux and Kirk 2014; Sadier et al. 2018), and eye position is related to activity pattern in primates (Heesy 2008). Larger olfactory bulbs support more expansive epithelia and therefore larger surface areas for odor detection (Barton et al. 1995; Buschhüter et al. 2008; Corfield et al. 2015), and enlarged olfactory epithelia are associated with frugivory among noctilionoid bats (Yohe et al. 2022). Cochlear volume and shape are correlated with aspects of cochlear morphology that influence hearing performance (Kössl and Vater 1995; Kirk and Gosselin-Ildari 2009; Vater and Kössl 2011; Davies et al. 2013*a*, 2013*b*). Our olfactory module encompassed landmarks placed on the impression of the olfactory bulb on the internal surface of the skull, we defined the cochlea module by landmarks placed on the region of the cranial base that encompasses the cochlea, and we delineated the eye module by landmarks placed on the surface of the reconstructed orbital sphere.

We defined five mechanical modules that encompass but do not directly measure elements of the masticatory system, whose shape and size affect bite force and a bat's ability to extract nectar from deep within the corollas of large flowers: the external cranial vault, palate, face, zygomatico-glenoid complex, and the cranial base (fig. 1; videos S1, S2). In using these modules, we assume that variation in their shapes reflects, at least in part, known functional variation in their constituent parts. For example, the external cranial vault provides the attachment area of the temporalis muscle, which generates the highest jaw-closing moments in bats that consume hard food items (hard fruits, vertebrates) and the lowest moments in nectar-feeding species (Santana et al. 2010, 2012).

Likewise, variation in the shape of the palate—and by association the face—is closely associated with the ability to generate bite force. Species with short, broad palates generate relatively higher bite forces for their size than species with long, narrow palates (Aguirre et al. 2002; Nogueira et al. 2009; Davis et al. 2010; Santana et al. 2010). In mechanical terms, shorter palates (and faces) increase mechanical advantage (Freeman and Lemen 2010), which is a target of selection in some phyllostomid bats and linked to an increase in speciation rate in fig specialists (Dumont et al. 2012, 2014). In contrast, elongated palates and faces support elongated tongues that increase the efficiency of extracting nectar from flowers, and there is evidence for the morphological specialization of different nectar-feeding species on flowers with different corolla depths (Paton and Collins 1989; Winter and von Helversen 2003; Gonzalez-Terrazas et al. 2012).

The zygomatico-glenoid complex carries two clear functional associations that we assume are reflected in our dataset. The first is the origin of the masseter muscle, which is the single best predictor of bite force in phyllostomids (Santana et al. 2012). The second is the temporomandibular joint. Its location relative to the molar toothrow (and palate) is associated with variation in diet among bats (Freeman 1979; Santana et al. 2012).

Finally, the relative position of the cranial base and palate are linked to whether bats emit echolocation calls through their mouths (oral emitters) or through their noses (nasal emitters; Pedersen 1993). The angle between the long axes of the cranial base and palate approaches 180° in oral emitters, while the angle is more acute in nasal emitters. Phyllostomids are nasal emitters and other noctilionoids are oral emitters, so we expect to see differences in the shape and/or orientation of the cranial base module between the two groups.

Testing Modularity Hypotheses

We tested one null and four functional modularity hypotheses (table S6). The null model proposes that eight modules are evolving in tandem as one unit. The first functional hypothesis (M1) addresses our first hypothesis, that all sensory modules are part of one module and all mechanical hypotheses are part of another. Support for this modularity hypothesis would be consistent with the idea that sensory and mechanical systems are each tightly integrated because their parts must be perfectly tuned to function together but that sensory and mechanical modules are not tightly integrated with one another. The second functional hypothesis (M2) is that the mammalian skull is divided into two functional modules, the neurocranium and the rostrum (face, palate, and eye modules combined). This hypothesis is supported by many studies and implies that the rostrum, the neurocranium, or the relationship between them is the locus of shape changes that affect functional diversity (e.g., Marroig et al. 2009; Porto et al. 2009; Santana and Lofgren 2013; Hedrick et al. 2020). The third functional hypothesis (M3) is that the face and palate constitute a single module and all other modules are separate and independent of one another. This hypothesis addresses the fact that dietary differentiation among phyllostomids is primarily driven by rostral elongation and shortening (Freeman 2000; Dumont et al. 2012; Hedrick et al. 2020). The fourth functional hypothesis (M4) proposes that all eight modules are independent of one another.

We tested the relative strength of these five modularity hypotheses using the EMMLi package in R (Goswami and Finarelli 2016), which uses a maximum likelihood approach to compare sets of modularity hypotheses and applies the Akaike information criterion corrected for small sample sizes. We implemented EMMLi for the dataset encompassing all noctilionoids and again after partitioning it into phyllostomids and nonphyllostomid noctilionoids. We quantified effect sizes using the modularity.test function within the geomorph package in R (Adams and Collyer 2019) to evaluate whether modularity differed significantly between the three partitions.

We also indirectly tested the independence of the resulting modules by comparing their rates of shape change using Bayestraits. First, we calculated the net rate of shape evolution of each module across all noctilionoids using geomorph in R with 1,000 random permutations under a Brownian motion (BM) model of evolution (Adams and Otárola-Castillo 2013) for the landmarks demarcating the shape of each module. We then tested whether these rates were significantly different across modules and between phyllostomids and other noctilionoids using the function compare.multi.evol.rates in geomorph (Denton and Adams 2015). This function compares net rates of morphological evolution for multidimensional traits under a BM model of evolution.

Visualizing Module Evolution

We visualized the evolution of shape in each module across all noctilionoids in three ways to observe patterns at three hierarchical scales: normalized average rates of shape evolution within successive slices of time, relative rates of shape evolution among lineages, and rates and directions of change in module shape.

The normalized average rates of shape evolution for each module plotted through time illustrates the average rate of each module's shape change across lineages within successive time bins relative to that module's maximum average evolutionary rate. This provides an overview of rate changes within modules over time relative to one another across all species within each time slice. We used reverse-jump Markov chain Monte Carlo within BayesTraits to account for lineage diversification and multivariate trait evolution (i.e., the use of multiple PCs; Meade and Pagel 2016). Using a variable rates model with the independent contrasts and autotune options, we ran 110 million iterations and discarded the first 10 million as burn-in. We plotted the rate through time using 1-million-year time bins from the best rate model (selected by BayesTraits) for each module using the BTR tools package in R (Ferguson-Gow 2017; see Felice et al. (2018). Following Felice et al. (2018), we adjusted the average rate across branches within each time bin by the maximum average rate attained for that module. We noted the timing of seven events associated with positive selection of visual genes and dietary changes (Davies et al. 2020): the last common ancestors of the Noctilionoidea, Mormoopidae, and Phyllostomidae as well as all plant-feeding phyllostomids, nectar-feeding Glossophaginae and Lonchophyllinae, and fig-eating Stenodermatinae.

We visually compared rates of evolution in module shape across the noctilionoid phylogeny by creating a "rate tree" for each module using the best-supported evolutionary model in BayesTraits. Each tree was scaled by its maximum rate. Comparing trees across modules can reveal lineage-specific patterns (e.g., correlated increases or decreases in evolutionary rates) that are obscured in the rate-through-time plot and highlights the extent to which the rate-through-time plot is influenced by a concentration of fast rates in a few lineages.

Finally, we visualized the evolution of module shape by plotting the first two PCs of shape variation across the phylogeny for each module. For this dataset, most of the variation was concentrated in the first + second PC (base = 63%, olfactory bulb = 71%, cochlea region = 72%, palate = 76%, face = 78%, external vault = 85%, eye = 88%, zygomatico-glenoid complex = 93%). The plots illustrate the direction of shape change as well as its rate and timing. Module shape is associated with module function, so qualitative comparisons of character states among modules can provide insights into how mechanical and sensory functions may—and may not—have changed in concert during noctilionoid evolution.

Evaluating Disparity and Integration

We tested the hypothesis that within each module the relationship between phenotypic disparity and rate of shape evolution differs significantly from a null Brownian model in a way that is consistent with either evolutionary facilitation or constraint. Average disparity for each module (Procrustes variance) was calculated from Procrustes distances of all its landmarks. The average rate of evolution of each module (σ) was calculated as the average of the sum of σ values of each of its coordinates (x, y, and z; Revell et al. 2008; Adams and Otárola-Castillo 2013). We plotted Procrustes variance within each module against the evolutionary rate (σ) for each landmark with the BM expectation of evolution of uncorrelated traits and used standardized major axis regressions to compare each module's regression against the BM slope using the R package smatr (Warton et al. 2012; Felice et al. 2018). Each module's slope was also compared against that of other modules.

To explore whether integration influences the disparity and evolutionary rate of module shape across all noctilionoids, we regressed the average rate of evolution (σ), average disparity (Procrustes variance), and average integration (ρ coefficient) against one other for each module. The ρ coefficient was derived from the EMMLi analysis.

Results

We found significant support for all eight mechanical and sensory modules within Noctilionoidea as well as within the subsets of phyllostomids and nonphyllostomid noctilionoids (table S7). All other hypotheses of modularity were rejected. The whole noctilionoid group (Zcr $= -13.5993 \pm 0.0110$ SE, $P = .002$), only phyllostomids (Zcr $= -13.1809 \pm 0.107$ SE, $P = .004$), and other noctilionoid species (Zcr $= -10.74024 \pm 0.0108$ SE, $P = .004$) all exhibited significant modularity.

Noctilionoids exhibited high within-module integration of the eye, zygomatico-glenoid complex, and face (diagonal values in fig. 2). Note that the eye's exceptionally high within-module integration values (0.95–0.99) are likely the result of fitting a sphere to the space. Almost all other structures have significantly lower integration values (within-module values on diagonal, 0.42–0.85, except for zygomatico-glenoid, which was 0.85–0.94). In general, between-module integration is of intermediate strength and evenly distributed, with similar levels of integration between and among sensory and mechanical modules (off-diagonal values in fig. 2). There is low integration between the eye and cranial base and between the olfactory bulb and both the cochlea and the zygomatico-glenoid complex. In contrast, the integration between the zygomatico-glenoid complex and the eye, external vault,

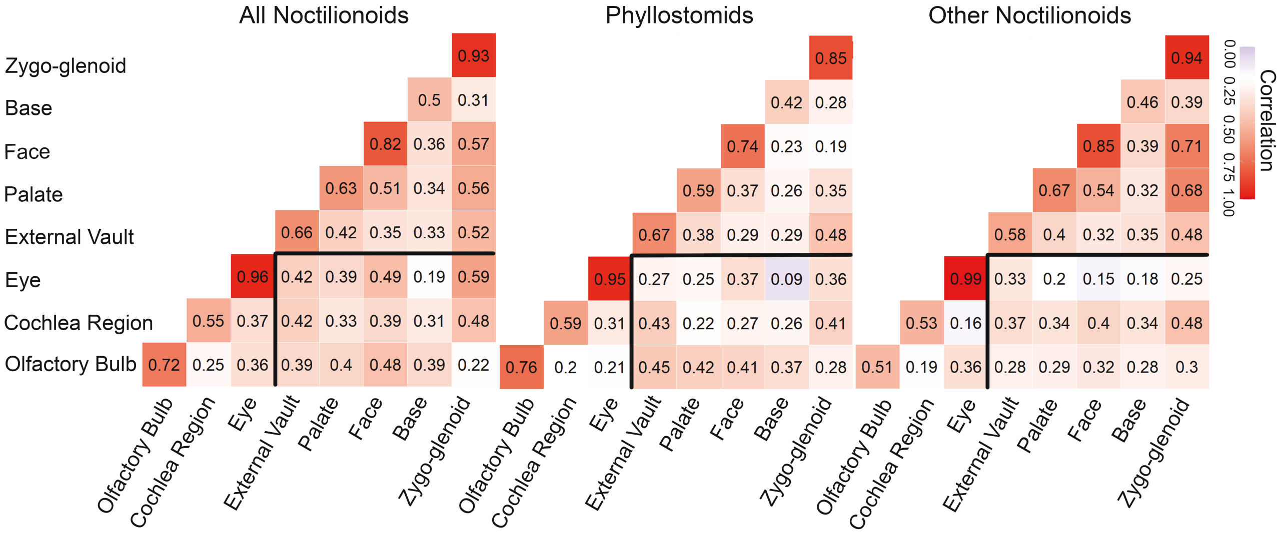

All Noctilionoids

	Olfactory Bulb	Cochlea Region	Eye	External Vault	Palate	Face	Base	Zygo-glenoid
Zygo-glenoid								0.93
Base							0.5	0.31
Face						0.82	0.36	0.57
Palate					0.63	0.51	0.34	0.56
External Vault				0.66	0.42	0.35	0.33	0.52
Eye			0.96	0.42	0.39	0.49	0.19	0.59
Cochlea Region		0.55	0.37	0.42	0.33	0.39	0.31	0.48
Olfactory Bulb	0.72	0.25	0.36	0.39	0.4	0.48	0.39	0.22

Phyllostomids

	Olfactory Bulb	Cochlea Region	Eye	External Vault	Palate	Face	Base	Zygo-glenoid
Zygo-glenoid								0.85
Base							0.42	0.28
Face						0.74	0.23	0.19
Palate					0.59	0.37	0.26	0.35
External Vault				0.67	0.38	0.29	0.29	0.48
Eye			0.95	0.27	0.25	0.37	0.09	0.36
Cochlea Region		0.59	0.31	0.43	0.22	0.27	0.26	0.41
Olfactory Bulb	0.76	0.2	0.21	0.45	0.42	0.41	0.37	0.28

Other Noctilionoids

	Olfactory Bulb	Cochlea Region	Eye	External Vault	Palate	Face	Base	Zygo-glenoid
Zygo-glenoid								0.94
Base							0.46	0.39
Face						0.85	0.39	0.71
Palate					0.67	0.54	0.32	0.68
External Vault				0.58	0.4	0.32	0.35	0.48
Eye			0.99	0.33	0.2	0.15	0.18	0.25
Cochlea Region		0.53	0.16	0.37	0.34	0.4	0.34	0.48
Olfactory Bulb	0.51	0.19	0.36	0.28	0.29	0.32	0.28	0.3

Figure 2: Integration within Noctilionoidea and its subdivision into phyllostomids and other noctilionoids. Within-module integration (diagonal values) and between-module integration (off-diagonal values) are expressed as ρ coefficients, calculated using EMMLi. The rectangle of blocks delineated by the black lines describes integration between mechanical and sensory modules. Integrations among mechanical modules are above the rectangles, and integrations among sensory modules are to the left of the rectangle. Warmer colors represent higher integration.

palate, and face is relatively high. Noctilionoidea as a group exhibits stronger integration among mechanical modules, among sensory modules, and between mechanical and sensory modules than both phyllostomids and nonphyllostomid noctilionoids.

The relatively uniform and strong integration within and between modules in Noctilionoidea masks distinct differences in within- and between-module integration (diagonal and off-diagonal values, respectively) between phyllostomids and nonphyllostomid noctilionoids. Within-module integration of the eye, zygomatico-glenoid complex, and face is strong within the two subgroups, echoing the pattern across Noctilionoidea (diagonal values in fig. 2). Among sensory modules, phyllostomids exhibit higher within-module integration of the olfactory bulb and, to a lesser extent, the cochlea. With respect to mechanical modules, phyllostomids exhibit higher integration of the external vault, while other noctilionoids exhibit higher within-module integration of the zygomatico-glenoid complex, face, and palate. The integration of the cranial base is similar across all three groups.

With respect to between-module integration, phyllostomids exhibit weaker relationships among mechanical modules and stronger relationships between sensory (eye and olfactory bulb) and mechanical modules than do nonphyllostomid noctilionoids (off-diagonal values in fig. 2). The integration of the eye and olfactory bulb is weaker, while the integration of the eye and the cochlea is stronger, in phyllostomids than in other noctilionoids. In contrast to phyllostomids, integration of mechanical modules is much higher among other noctilionoids. The olfactory bulb is more strongly integrated with mechanical modules in phyllostomids, as is the integration of the eye with the palate, face, and zygomatico-glenoid complex. In contrast, the cochlea is more strongly integrated with most mechanical modules in nonphyllostomid noctilionoids. The exception is the external vault, which is more closely tied to the cochlea in phyllostomids. Overall, the average strength of integration among sensory module and mechanical module subsets is similar within phyllostomids (mean $\rho = 0.31$) and other noctilionoids (mean $\rho = 0.30$), while mechanical modules are almost twice as integrated as sensory modules among other noctilionoids (mean $\rho = 0.46$) than in phyllostomids (mean $\rho = 0.25$).

In support of the hypothesis that modules evolved at different rates, we found substantial heterogeneity in net rates of evolution among sensory and mechanical modules for all noctilionoids, within phyllostomids, and within nonphyllostomid noctilionoids (table S8). On average, phyllostomids have a higher mean rate of module evolution (7.62E−07 ± 1.90E−07 σ^2mult) than other noctilionoids (5.13E−07 ± 1.43E−07 σ^2mult). The fastest-evolving module in both groups is the external cranial vault, followed by the face in phyllostomids and the zygomatico-glenoid complex in other noctilionoids. The slowest-evolving module in both phyllostomids and other noctilionoids is the eye, followed by the cochlea in other noctilionoids and the palate in phyllostomids. There are a few differences in mean rates of evolution between mechanical modules within phyllostomids and within other noctilionoids, but no significant differences among sensory modules. The rate of evolution of the external cranial vault is significantly higher than the palate in both groups, and the rate of evolution of the face is significantly higher than that of the palate in other noctilionoids. Several mechanical modules evolve significantly faster than the eye: the external cranial vault and face modules in both subgroups and the zygomatico-glenoid complex in phyllostomids.

The most striking pattern among rates of module evolution through time is that rates of evolution of sensory modules tend to peak earlier than those of mechanical modules (fig. 3). Among sensory modules, early increases in the evolutionary rates of the eye and cochlea modules preceded those of the olfactory module, which subsequently increased just before the emergence of the Mormoopidae. All three sensory modules attained peak rates before the divergence of the phyllostomids and slowed since. Mechanical modules also exhibit rate increases immediately preceding the divergence of the phyllostomids, but only the zygomatico-glenoid complex and the face modules reach their peak rates at that time. There is more disparity in rates of mechanical module evolution after the origin of phyllostomids, and the peak rates for the palate, external vault, and skull base modules are very close to the present. The short-faced stenodermatines and the long-faced glossophagines represent the two extremes of cranial morphology among phyllostomids, and there are concerted decreases in the rates of evolution of the face, zygomatico-glenoid, and external cranial vault occurring just prior to the origin of both clades. The rate of evolution of the palate module increases just before the appearance of the stenodermatine ancestor. In sum, the rates of sensory module evolution peak before the origin of phyllostomids and then decline steadily over time. In contrast, rates of mechanical module evolution peak either before the origins of phyllostomids or very recently and are far more variable throughout the evolution of noctilionoids.

Figure 4 illustrates relative rates of module evolution across the phylogeny and showcases rate heterogeneity among lineages. While figure 3 illustrates that peak mean

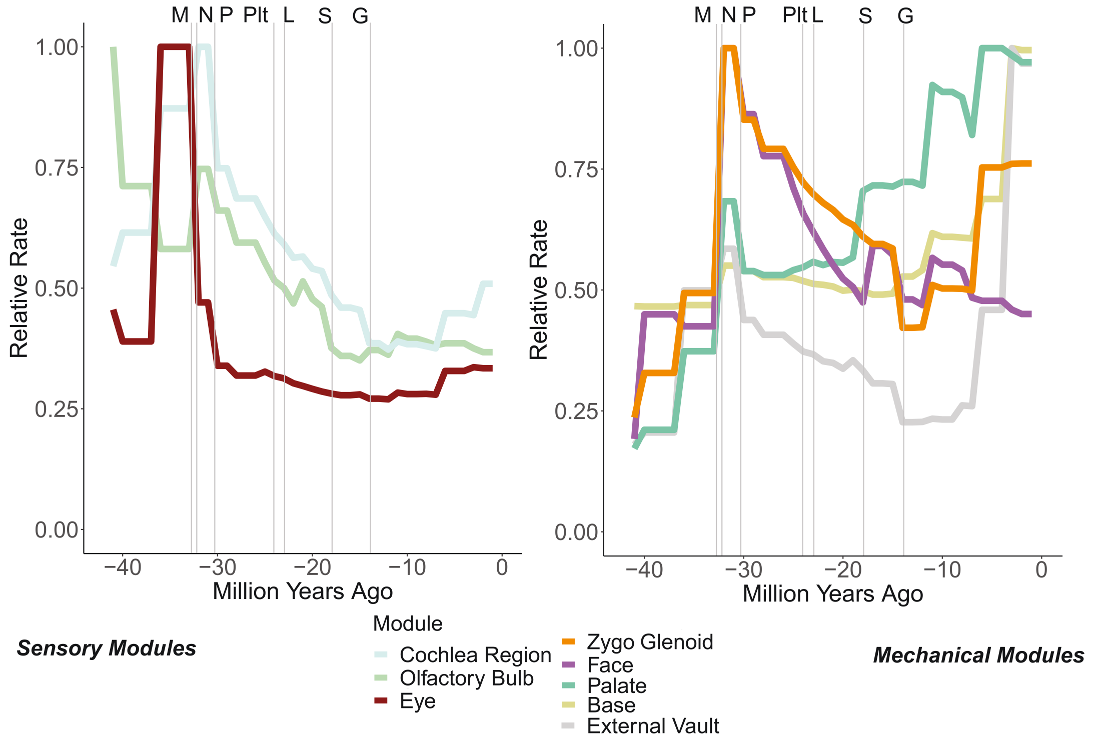

Figure 3: Evolutionary rate of each module plotted against time for sensory modules (*left*) and mechanical modules (*right*). Vertical lines denote the location of nodes associated with positively selected visual genes (Davies et al. 2020): the ancestor of Mormoopidae (M), the ancestor of Noctilionidae (N), the ancestor of Phyllostomidae (P), the origin of plant feeding within phyllostomids (Plt), the ancestor of the nectar-feeding Lonchophyllinae (L), the ancestor of the fig-eating Stenodermatinae (S), and the ancestor of the nectar-feeding Glossophaginae (G).

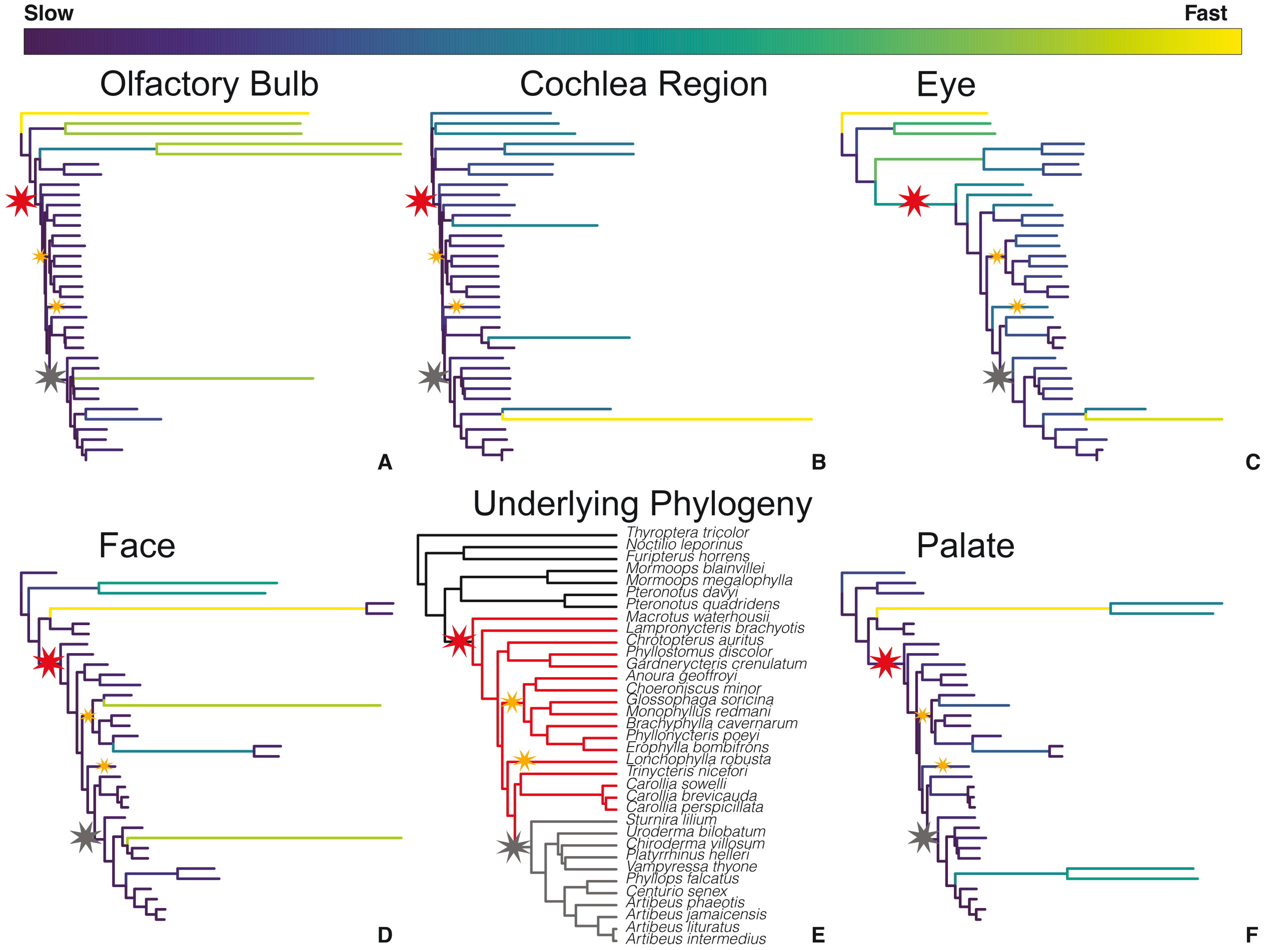

Figure 4: Evolutionary rates of sensory (*A–C*) and mechanical (*D*, *F*) modules mapped onto the phylogeny. Branch lengths are scaled by rates of evolution. Cool colors indicate low rates, and warm colors indicate high rates. Red stars indicate the origin of phyllostomids, orange stars indicate the origins of nectarivory, and gray stars indicate the origin of the fig-eating stenodermatines. *E* illustrates the underlying phylogeny. Evolutionary rates for the other mechanical modules are in figure S1).

evolutionary rates of sensory modules preceded those of some mechanical modules when lineages are combined in successive time bins, figures 4 and S1 (figs. S1–S8 are available online) illustrate the influence of individual taxa in driving that pattern. For example, some of the highest rates of sensory module evolution occur in the earliest lineages. Comparing rates of module evolution reveals several instances of parallel rate shifts that suggest correlated change. The eye is the sensory module with the most evenly distributed rates across the phylogeny, and its rapid evolution at the base of phyllostomids is accompanied by modest rate changes in all mechanical modules. Similarly, rates of olfactory bulb evolution are low along the backbone of the tree but exhibit a small increase at the base of the fig-feeding stenodermatines, perhaps in concert with rate increases in the eye, palate, cranial base, and external cranial vault modules. There are marked increases in the evolutionary rate of the eye and face modules in the branch leading to the hairy big-eyed bat, *Chiroderma villosum*. Among mechanical modules, there are correlated increases in the rates of face and palate module evolution in lineages ancestral to nectar feeders. Patterns of rate change are similar among the zygomatico-glenoid complex, external vault, and cranial base, with the latter two exhibiting high rates of evolution in the lineage ancestral to the Jamaican fruit bat, *Artibeus jamaicensis*.

By illustrating the rate, direction of changes, and range of shapes captured in the first two PCs of shape for each module across the phylogeny, figures 5 and S2–S7 offer the most nuanced pictures of module evolution. While variation in shape captured by PC1 separates phyllostomids from nonphyllostomid noctilionoids, PC2 separates

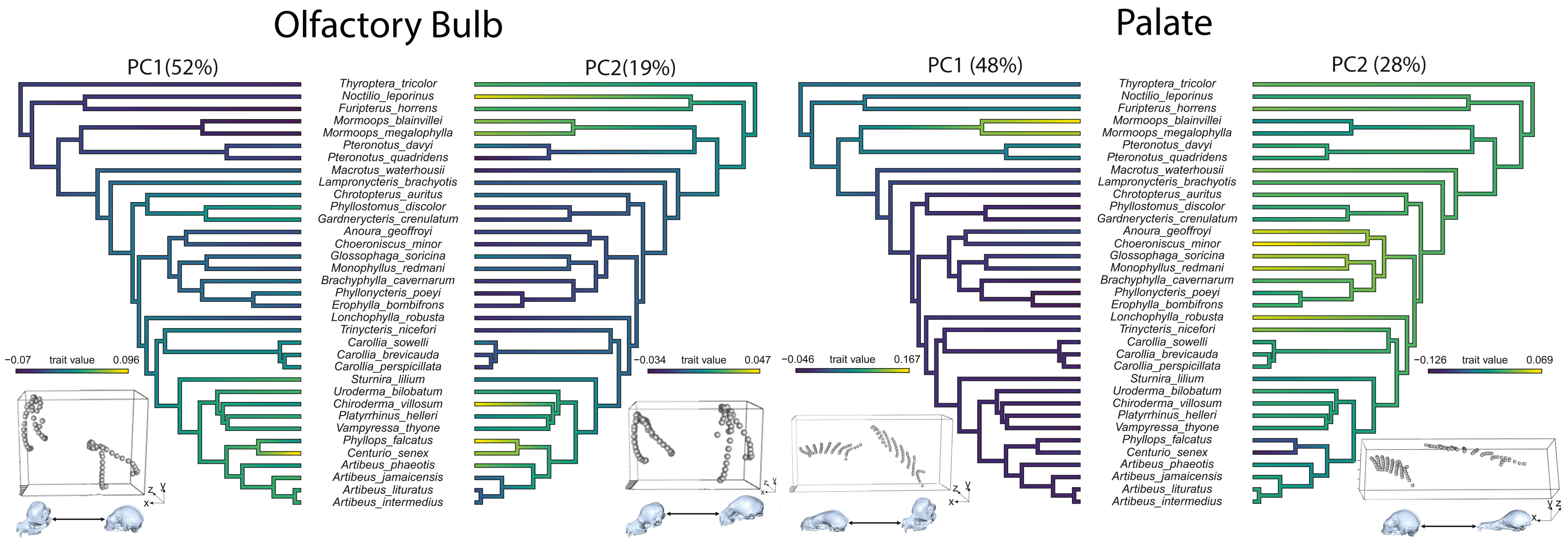

Figure 5: The first two principal components (PC1 and PC2) of olfactory bulb and palate module shapes across noctilionoids and their sister taxa. Percentages illustrate the proportion of variance explained by each component, and colors represent PC values. The crania and associated boxes of 3D landmarks illustrate the changes in the distribution of landmarks at the extremes of each PC.

taxa according to dietary guild and lineage. In most cases nectarivores are clearly distinguished from their sister taxa along PC2, with high values for some modules (palate, cochlea, eye, cranial base, zygomatico-glenoid, and palate) and low values for others (olfactory bulb, external vault, and face). PC2 values for the fig-feeding sternodermatines as a group are less distinct than those of nectar feeders. Instead, extreme PC2 values are common in the most short-faced species (*Phyllops falcatus* and *Centurio senex*) and, for the face and olfactory bulb modules, the big-eyed bat *Chiroderma villosum*. The morphologically intermediate nonphyllostomid noctilionoids exhibit intermediate PC2 values for most modules. As a reminder that our analyses include an element of size (we did not adjust for allometry), the PCs of eye shape (fig. S2) reflect variation in the size of the eye as well as its position in space.

Our third hypothesis was that the relationship between phenotypic disparity and rate of evolution departs from the Brownian model within each module (Felice et al. 2018). We expected sensory modules to have significantly lower slopes than the null model, indicative of constraint, and mechanical modules to have significantly higher slopes, suggesting that modularity facilitated diversification of trait values, especially among phyllostomids. Consistent with these expectations, we found significantly lower than predicted slopes for all three sensory modules within phyllostomids (table 1). The slope for the eye was also lower than predicted among nonphyllostomid noctilionoids, but the slope of the olfactory bulb was significantly higher. Among the mechanical modules, two were significantly lower among phyllostomids (base and external vault), while three of the five were significantly higher in nonphyllostomid noctilionoids (external vault, palate, and face). Overall, we found evidence for evolutionary constraint and selection, but not always in the ways we predicted (table S9).

Finally, we explored the relationship between integration and disparity and between integration and evolutionary rate across all noctilionoids (fig. S8). Across modules, disparity rises with increasing evolutionary rate ($R = 0.63$, $P < .01$), and the zygomatico-glenoid complex and external vault are the fastest evolving and most disparate. There is no evidence of a relationship between integration and either the rate of module evolution ($R = -0.14$, $P = .91$) or module disparity ($R = -0.13$, $P = .86$).

Discussion

By investigating two sets of functional modules whose relationships are largely unexplored—sensory modules that receive cues crucial to foraging and mechanical modules that contribute to bite force—we identified hitherto-unsuspected patterns of evolutionary change. First, instead of two suites of modules (sensory and mechanical), we found eight functional modules with varying rates of evolution that could have provided noctilionoids with a complex and rich stage on which selection could act (fig. 2; table S6, S7). In this system, disparity emerges from differential rates of evolution across mechanical and sensory modules (fig. 3; table S8) rather than from variation in modularity itself (fig. S8). Integration of some sensory and mechanical modules (fig. 2) as well as coordinated rate changes (figs. 3, 4, S1) imply that the two systems evolved synergistically, thereby linking abilities to sense and process novel foods. For example, phyllostomids are characterized by a newly evolved linkage between mechanical modules and the olfactory bulb and eye and a release from the association

Table 1: Results from a major axis regression comparing the observed variance-rate relationships (*P* values in columns) to the relationship predicted under Brownian motion (BM) evolution of uncorrelated traits

	All Neotropical noctilionoids				Phyllostomids				Other noctilionoids			
Type, module	Slope	Lower	Upper	*P*	Slope	Lower	Upper	*P*	Slope	Lower	Upper	*P*
BM null	.30	.30	.32		.26	.25	.27		.31	.29	.33	
Sensory:												
Eye	.39	.30	.49	.058	.13*	.11	.16	<.001	.16*	.14	.18	<.001
Olfactory bulb	.14*	.11	.18	<.001	.06*	.04	.07	<.001	.52*	.44	.61	<.001
Cochlea	.16*	.13	.18	<.001	.07*	.06	.09	<.001	.26	.24	.29	.832
Mechanical:												
Base	.12*	.09	.17	<.001	.09*	.06	.12	<.001	.37	.26	.53	.068
External vault	.32	.25	.40	.666	−.13*	−.19	−.08	.002	.55*	.52	.59	<.001
Palate	.37*	.33	.40	<.001	.24	.22	.27	.327	.65*	.59	.73	<.001
Zygomatico-glenoid	.22	.05	.92	.532	.09	.02	.55	.207	.38	.16	.89	.236
Face	.38	.30	.47	.057	.31	.26	.37	.09	.34*	.29	.41	.004

[*] $P < .05$ for the difference between the BM and module slopes.

between mechanical modules and the cochlea (fig. 2). From a functional perspective, the coupling of mechanical modules with the visual and olfactory systems is consistent with a shift to foraging for plants, which relies more heavily on vision and olfaction than aerial insectivory. The timing of this change (fig. 3) indicates that the shift in the evolution of sensory modules predated most changes in mechanical modules, supporting a sensory-first hypothesis of diversification. We propose shifts in evolutionary rates influenced integration among modules, likely opening new dietary niches and providing the structural flexibility necessary for the radiation of noctilionoid bats.

Our work provides a more holistic perspective on functional ecology than previous analyses of modularity and integration. While Hedrick et al.'s (2020) two-module hypothesis found that phyllostomids were twice as integrated but more disparate than other noctilionoids, this finer-scale partitioning of the cranium into eight modules suggests that phyllostomids are less integrated. The strength of integration within mechanical and sensory modules is similar and relatively low within phyllostomids. In contrast, the strength of integration within mechanical modules is high and nearly twice as strong as that of sensory modules in other noctilionoids. We propose that considering multiple functional modules and their relationships to one another offers a more robust insight into the context for diversification than do analyses of fewer functional modules.

Although the reorganization of the phyllostomid cranium has received a great deal of attention (e.g., Freeman 2000; Dumont et al. 2012), much less is known about the noctilionoid cranium (Hedrick et al. 2020). The rate-through-time plot (fig. 3) reveals mosaic evolution of module shape across Noctilionoidea, involving both phyllostomids and other noctilionoids. While previous analyses found high rates of cranial mechanical evolution within phyllostomids (Dumont et al. 2012, 2014), rate trees for each module reveal faster rates of module evolution in lineages that predate the origin of phyllostomids (figs. 4, S1). Analyses of character state evolution provide the clearest picture of correlated structural change both outside and within Phyllostomidae (figs. 5, S2–S7). For the olfactory bulb, the major axis of variation (PC1) evolves fastest within phyllostomids, stenodermatines in particular. Shape change is more evenly distributed along PC2. For the palate, shape changes along PC1 separate phyllostomids from other noctilionoids, while PC2 separates dietary guilds among phyllostomids, especially nectarivores.

Our results align with the view that preadaptation in sensory systems played a leading role in the evolution of bats (Thiagavel et al. 2018; Davies et al. 2020) and the earliest phyllostomids experimented with foods beyond insects (Freeman 2000; Baker et al. 2012; Hedrick et al. 2020) while also demonstrating how sensory and mechanical abilities coevolve. Just before the appearance of the phyllostomid ancestor (fig. 3), rate changes in sensory and mechanical modules occurred in concert, involving the face, zygomatico-glenoid complex, palate, and external vault, but the cochlea and olfactory bulb evolved most quickly. As a result, phyllostomids are characterized by a larger olfactory bulb that occupies relatively more space as well as alignment between the palate and cranial base (figs. 5, S2–S7). Both changes are consistent with a plant-based diet requiring higher odor acuity (Barton et al. 1995; Buschhüter et al. 2008; Corfield et al. 2015) and the shift from oral to nasal emission of echolocation sounds (Pedersen 1993). Within phyllostomids, module coevolution supports more specialized behaviors, such as the ability to detect flowers and ripe fruits and to process nectar and hard fruits (Davies et al. 2013*a*, 2013*b*, 2020; Thiagavel et al. 2018). Nectar-feeding lineages exhibit elevated rates of evolution in the palate, face, and, to a lesser extent, the skull base and eye modules (figs. 4, S1). The results are elongated narrow skulls and palates that can reach into the corollas of flowers (figs. 5, S2–S7) and the repositioning of the eye (fig. S2). The fruit-specialist Stenodermatine bats have short, broad faces and stout crania, expanded olfactory bulb, enlarged eyes, and more robust zygomatic arches (figs. 5, S2–S7).

By identifying multiple functional modules and their interrelationships, our work demonstrates how parallel changes in sensory and mechanical modules were associated with the ecomorphological diversification in this clade. Rather than arising from ecological opportunity alone, we propose that intrinsic changes in morphological structure—modularity, integration, and the rates and timing of evolution among mechanical and sensory modules—also contribute to the explosive ecological and phenotypic radiation of phyllostomids. Exposed to similar ecological conditions in the Neotropics, none of the other six families of resident bats exhibit high phenotypic disparity or species diversity. The ancestor of phyllostomids was distinguished by simultaneous changes in the evolutionary rates of the zygomatico-glenoid complex, face, olfactory bulb, and cochlea that are not associated with changes in the degree of within-module integration (fig. S8). Instead, phenotypic innovation emerged through variable rates of evolution among modules that resulted in different combinations of sensory and mechanical functions over time. Coordination of corresponding functions, such as changes in bite force, olfaction, and echolocation, provided the phyllostomid ancestor with the ability to diversify into available plant-based niches. We therefore propose that the phyllostomid radiation was facilitated by structural opportunity—variation in the rate and timing of change in functional structures—in addition to ecological opportunity. Therefore, ecology alone cannot explain radiation: the underlying morphological structures, correlations among those structures, and their functions also impact the nature of an organism's relationship with its environment.

Acknowledgments

We thank Greg Lin and Jim Reynolds for access to the micro-CT scanner used in this study and for technical support. This work was performed in part at the Center for Nanoscale Systems (CNS), a member of the National Nanotechnology Coordinated Infrastructure Network, which is supported by the National Science Foundation under award ECS-1541959. For access to specimens, we thank the American Museum of Natural History and the Yale Peabody Museum. We thank Ryan Felice and Robin Trayler for help with R coding. This project was made possible by funding from the National Science Foundation (PRFB-1612211, DEB-1442142, DEB-1442314, and DEB-1442278).

Statement of Authorship

G.L.M., B.P.H., R.P.H., and E.R.D. conceived the idea for this study. G.L.M., B.P.H., and R.P.H. collected data for analysis. G.L.M. performed all analyses with guidance from E.R.D., B.P.H. and R.P.H. E.R.D. and L.M.D. contributed substantial guidance throughout the project. All authors contributed ideas and assisted with the writing process.

Data and Code Availability

The data that support the findings of this study are openly available in the Dryad Digital Repository (https://doi.org/10.5061/dryad.x95x69pmx; Mutumi et al. 2023). The repository has five files; the main dataset of all landmarks used, MasterMeanShapes_latest_newnames; the pruned phylogeny of Noctilionoids used in this study, battree.nexus; the modularity hypothesis CVS file Modules_FromRtt; a text document with a few guidelines, README_BatSkullModules.Fin; and an Excel spreadsheet table with results from a test for the sensitivity of our landmarking density, S4 Table_Sensitivity_Test_AmNat_. Note that these files are not exhaustive of the whole analysis but provide the basics. For detailed information, contact the authors.

Literature Cited

Adams, D. C., and M. L. Collyer. 2019. Comparing the strength of modular signal, and evaluating alternative modular hypotheses, using covariance ratio effect sizes with morphometric data. Evolution 1902511:2352–2367.

Adams, D. C., and E. Otárola-Castillo. 2013. geomorph: an R package for the collection and analysis of geometric morphometric shape data. Methods in Ecology and Evolution 4:393–399.

Aguirre, L. F., A. Herrel, R. van Damme, and E. Matthysen. 2002. Ecomorphological analysis of trophic niche partitioning in a tropical savannah bat community. Proceedings of the Royal Society B 269:1271–1278.

Arbour, J. H., A. A. Curtis, and S. E. Santana. 2019. Signatures of echolocation and dietary ecology in the adaptive evolution of skull shape in bats. Nature Communications 10:2036.

Arlegi, M., A. Gómez-Robles, and A. Gómez-Olivencia. 2018. Morphological integration in the gorilla, chimpanzee, and human neck. American Journal of Physical Anthropology 166:408–416.

Assis, A. P. A., D. M. Rossoni, J. L. Patton, and G. Marroig. 2016. Evolutionary processes and its environmental correlates in the cranial morphology of western chipmunks (*Tamias*). Evolution 71:595–609.

Atchley, W. R., and B. K. Hall. 1991. A model for development and evolution of complex morphological structures. Biological Reviews of the Cambridge Philosophical Society 66:101–157.

Baker, R. J., O. R. P. Bininda-Emonds, H. Mantilla-Meluk, C. A. Porter, and R. A. Van Den Bussche. 2012. Molecular timescale of diversification of feeding strategy and morphology in New World Leaf-Nosed Bats (Phyllostomidae): a phylogenetic perspective. Pages 385–409 *in* G. F. Gunnell and N. B. Simmons, eds. Evolutionary history of bats: fossils, molecules and morphology. Cambridge University Press, Cambridge.

Bardua, C., M. Wilkinson, D. J. Gower, E. Sherratt, and A. Goswami. 2019. Morphological evolution and modularity of the caecilian skull. BMC Evolutionary Biology 19:1–23.

Barton, R. A., A. Purvis, and P. H. Harvey. 1995. Evolutionary radiation of visual and olfactory brain systems in primates, bats and insectivores. Philosophical Transactions of the Royal Society B 348:381–392.

Bookstein, F. L. 1997. Landmark methods for forms without landmarks: morphometrics of group differences in outline shape. Medical Image Analysis 1:225–243.

Buschhüter, D., M. Smitka, S. Puschmann, J. C. Gerber, M. Witt, N. D. Abolmaali, and T. Hummel. 2008. Correlation between olfactory bulb volume and olfactory function. Neuroimage 42:498–502.

Conith, A. J., S. A. Hope, B. H. Chhouk, and R. C. Albertson. 2021. Weak genetic signal for phenotypic integration implicates developmental processes as major regulators of trait covariation. Molecular Ecology 30:464–480.

Conith, A. J., D. T. Lam, and R. C. Albertson. 2019. Muscle-induced loading as an important source of variation in craniofacial skeletal shape. Genesis 57:1–13.

Corfield, J. R., K. Price, A. N. Iwaniuk, C. Gutiérrez-Ibáñez, T. Birkhead, and D. R. Wylie. 2015. Diversity in olfactory bulb size in birds reflects allometry, ecology, and phylogeny. Frontiers in Neuroanatomy 9:102.

Cumming, G. S., D. H. M. Cumming, and C. L. Redman. 2006. Scale mismatches in social-ecological systems. Ecology and Society 11:14.

Davidson, E. 2010. Leader for DB "Developmental Gene Regulatory Networks" collection. Developmental Biology 340:160.

Davies, K. T. J., P. J. J. Bates, I. Maryanto, J. A. Cotton, and S. J. Rossiter. 2013*a*. The evolution of bat vestibular systems in the face of potential antagonistic selection pressures for flight and echolocation. PLoS ONE 8:e61998.

Davies, K. T. J., I. Maryanto, and S. J. Rossiter. 2013*b*. Evolutionary origins of ultrasonic hearing and laryngeal echolocation in bats inferred from morphological analyses of the inner ear. Frontiers in Zoology 10:2.

Davies, K. T. J., L. R. Yohe, J. Almonte, M. K. R. Sánchez, E. M. Rengifo, E. R. Dumont, K. E. Sears, et al. 2020. Foraging shifts and visual preadaptation in ecologically diverse bats. Molecular Ecology 29:1839–1859.

Davis, J. L., S. E. Santana, E. R. Dumont, and I. R. Grosse. 2010. Predicting bite force in mammals: two-dimensional versus three-dimensional lever models. Journal of Experimental Biology 213:1844–1851.

Denton, J. S. S., and D. C. Adams. 2015. A new phylogenetic test for comparing multiple high-dimensional evolutionary rates suggests interplay of evolutionary rates and modularity in lanternfishes (Myctophiformes; Myctophidae). Evolution 69:2425–2440.

Dumont, E. R. 2004. Patterns of diversity in cranial shape among plant-visiting bats. Acta Chiropterologica 6:59–74.

Dumont, E. R., L. M. Dávalos, A. Goldberg, S. E. Santana, K. Rex, C. C. Voigt, E. R. Dumont, et al. 2012. Morphological innovation, diversification, and invasion of a new adaptive zone. Proceedings of the Royal Society B 279:1797–1805.

Dumont, E. R., A. Herrel, R. A. Medellín, J. A. Vargas-Contreras, and S. E. Santana. 2009. Built to bite: cranial design and function in the wrinkle-faced bat. Journal of Zoology 279:329–337.

Dumont, E. R., K. Samadevam, I. Grosse, O. M. Warsi, B. Baird, and L. M. Davalos. 2014. Selection for mechanical advantage underlies multiple cranial optima in new world leaf-nosed bats. Evolution 68:1436–1449.

Eklöf, J., J. Šuba, G. Petersons, and J. Rydell. 2014. Visual acuity and eye size in five European bat species in relation to foraging and migration strategies. Environmental and Experimental Biology 12:1–6.

Erwin, D. H., and E. H. Davidson. 2009. The evolution of hierarchical gene regulatory networks. Nature Reviews Genetics 10:141–148.

Esteve-altava, B. 2017. In search of morphological modules: a systematic review. Biological Reviews 92:1332–1347.

Evans, K. M., O. Larouche, S.-J. Watson, S. Farina, M. L. Habegger, and M. Friedman. 2021. Integration drives rapid phenotypic evolution in flatfishes. Proceedings of the National Academy of Sciences of the USA 118:e2101330118.

Evans, K. M., B. Waltz, V. Tagliacollo, P. Chakrabarty, and J. S. Albert. 2017. Why the short face? developmental disintegration of the neurocranium drives convergent evolution in neotropical electric fishes. Ecology and Evolution 7:1783–1801.

Felice, R. N., and A. Goswami. 2017. Developmental origins of mosaic evolution in the avian cranium. Proceedings of the National Academy of Sciences of the USA 115:555–560.

Felice, R. N., M. Randau, and A. Goswami. 2018. A fly in a tube: macroevolutionary expectations for integrated phenotypes. Evolution 72:2580–2594.

Ferguson-Gow, H. 2017. BTRTools: a set of tools for processing and analysing the output of BayesTraits. GitHub.

Fleming, T. H., L. M. Dávalos, and M. A. R. Mello. 2020. Phyllostomid bats: a unique mammalian radiation. University of Chicago Press, Chicago.

Freeman, P. W. 1979. Specialized insectivory: beetle-eating and moth-eating molossid bats. Journal of Mammalogy 60:467–479.

———. 2000. Macroevolution in Microchiroptera: recoupling morphology and ecology with phylogeny. Evolutionary Ecology Research 2:317–335.

Freeman, P. W., and C. A. Lemen. 2010. Simple predictors of bite force in bats: the good, the better and the better still. Journal of Zoology 282:284–290.

Gignac, P. M., N. J. Kley, J. A. Clarke, M. W. Colbert, A. C. Morhardt, D. Cerio, I. N. Cost, et al. 2016. Diffusible iodine-based contrast-enhanced computed tomography (diceCT): an emerging tool for rapid, high-resolution, 3-D imaging of metazoan soft tissues. Journal of Anatomy 228:889–909.

Gonzalez-Terrazas, T. P., R. A. Medellin, M. Knörnschild, and M. Tschapka. 2012. Morphological specialization influences nectar extraction efficiency of sympatric nectar-feeding bats. Journal of Experimental Biology 215:3989–3996.

Goswami, A. 2006. Cranial modularity shifts during mammalian evolution. American Naturalist 168:270–280.

Goswami, A., and J. A. Finarelli. 2016. EMMLi: a maximum likelihood approach to the analysis of modularity. Evolution 70:1622–1637.

Goswami, A., and P. D. Polly. 2010. The influence of modularity on cranial morphological disparity in carnivora and primates (Mammalia). PLoS ONE 5:e9517.

Goswami, A., J. B. Smaers, C. Soligo, and P. D. Polly. 2014. The macroevolutionary consequences of phenotypic integration: from development to deep time. Philosophical Transactions of the Royal Society B 369:20130254.

Gould, S. J., and R. T. Lewontin. 1979. The spandrels of San Marco and the Panglossian paradigm. Proceedings of the Royal Society B 205:581–598.

Gunz, P., and P. Mitteroecker. 2013. Semilandmarks: a method for quantifying curves and surfaces. Hystrix 24:103–109.

Hall, R. P., G. L. Mutumi, B. P. Hedrick, L. R. Yohe, A. Sadier, K. T. J. Davies, L. M. Dávalos, et al. 2021. Find the food first: an omnivorous sensory morphotype predates biomechanical specialization for plant based diets in phyllostomid bats. Evolution 75:2791–2801.

Hedrick, B. P., and E. R. Dumont. 2018. Putting the leaf-nosed bats in context: a geometric morphometric analysis of three of the largest families of bats. Journal of Mammalogy 99:1042–1054.

Hedrick, B. P., G. L. Mutumi, R. P. Hall, D. V. Munteanu, A. Sadier, K. T. J. Davies, S. J. Rossiter, et al. 2020. Morphological diversification under high integration in a hyper diverse mammal clade. Journal of Mammalian Evolution 27:563–575.

Heesy, C. P. 2008. Ecomorphology of orbit orientation and the adaptive significance of binocular vision in primates and other mammals. Brain, Behavior and Evolution 71:54–67.

Hu, Y., L. Ghigliotti, M. Vacchi, E. Pisano, H. W. Detrich, and R. C. Albertson. 2016. Evolution in an extreme environment: developmental biases and phenotypic integration in the adaptive radiation of antarctic notothenioids. BMC Evolutionary Biology 16:142.

Jones, K. E., L. Benitez, K. D. Angielczyk, and S. E. Pierce. 2018. Adaptation and constraint in the evolution of the mammalian backbone. BMC Evolutionary Biology 18:172.

Kirk, E. C., and A. D. Gosselin-Ildari. 2009. Cochlear labyrinth volume and hearing abilities in primates. Anatomical Record 292:765–776.

Klingenberg, C. P. 2010. Evolution and development of shape: integrating quantitative approaches. Nature Reviews Genetics 11: 623–635.

Kössl, M., and M. Vater. 1995. Cochlear structure and function in bats. Pages 191–234 *in* A. N. Popper and R. R. Fay, eds. Hearing by bats. Springer, New York.

Land, M. F., and D.-E. Nilsson. 2012. Animal eyes. Oxford University Press, Oxford.

Mallarino, R., P. R. Grant, B. R. Grant, A. Herrel, W. P. Kuo, and A. Abzhanov. 2011. Two developmental modules establish 3D beak-shape variation in Darwin's finches. Proceedings of the National Academy of Sciences of the USA 108:4057–4062.

Marroig, G., L. T. Shirai, A. Porto, F. B. de Oliveira, and V. De Conto. 2009. The evolution of modularity in the mammalian skull II: evolutionary consequences. Evolutionary Biology 36: 136–148.

Meade, A., and M. Pagel. 2016. BayesTraits V3 81.

Müller, B., S. M. Goodman, and L. Peichl. 2007. Cone photoreceptor diversity in the retinas of fruit bats (Megachiroptera). Brain, Behavior and Evolution 70:90–104.

Müller, B., and L. Peichl. 2005. Retinal cone photoreceptors in microchiropteran bats. Investigative Ophthalmology and Visual Science 46:2259.

Mutumi, G. L., R. Hall, B. P. Hedrick, L. R. Yohe, A. Sadier, K. T. J. Davies, L. M. Dávalos, et al. 2023. Data from: Disentangling mechanical and sensory modules in the radiation of noctilionoid bats. American Naturalist, Dryad Digital Repository, https://doi.org/10.5061/dryad.x95x69pmx.

Neaux, D., B. Blanc, K. Ortiz, Y. Locatelli, F. Laurens, I. Baly, C. Callou, et al. 2021. How changes in functional demands associated with captivity affect the skull shape of a wild boar (*Sus scrofa*). Evolutionary Biology 48:27–40.

Nogueira, M. R., A. L. Peracchi, and L. R. Monteiro. 2009. Morphological correlates of bite force and diet in the skull and mandible of phyllostomid bats. Functional Ecology 23:715–723.

Paton, D. C., and B. G. Collins. 1989. Bills and tongues of nectar-feeding birds: a review of morphology, function and performance, with intercontinental comparisons. Australian Journal of Ecology 14:473–506.

Pedersen, S. C. 1993. Cephalometric correlates of echolocation in the Chiroptera. Journal of Morphology 218:85–98.

Porto, A., F. B. de Oliveira, L. T. Shirai, V. De Conto, and G. Marroig. 2009. The evolution of modularity in the mammalian skull I: morphological integration patterns and magnitudes. Evolutionary Biology 36:118–135.

Revell, L. J., L. J. Harmon, and D. C. Collar. 2008. Phylogenetic signal, evolutionary process, and rate. Systematic Biology 57:591–601.

Rodriguez-Durán, A., and J. Rosa. 2020. Remarkable variation in the diet of *Noctilio leporinus* in Puerto Rico: the fishing bat turns carnivorous. Acta Chiropterologica 22:175–178.

Rojas, D., O. M. Warsi, and L. M. Dávalos. 2016. Bats (Chiroptera: Noctilionoidea) challenge a recent origin of extant neotropical diversity. Systematic Biology 65:432–448.

Rolfe, A. K. 2011. Diet of three mormoopid bats (*Mormoops blainvillei*, *Pteronotus quadridens*, and *Pteronotus portoricensis*) on Puerto Rico. Master's Theses and Doctoral Dissertations. 349. http://commons.emich.edu/theses/349.

Rossoni, D. M., B. M. A. Costa, N. P. Giannini, and G. Marroig. 2019. A multiple peak adaptive landscape based on feeding strategies and roosting ecology shaped the evolution of cranial covariance structure and morphological differentiation in phyllostomid bats. Evolution 73:961–981.

Sadier, A., K. T. J. Davies, L. R. Yohe, K. Yun, P. Donat, B. P. Hedrick, E. R. Dumont, et al. 2018. Multifactorial processes underlie parallel opsin loss in neotropical bats. eLife 7:e37412.

Santana, S. E., E. R. Dumont, and J. L. Davis. 2010. Mechanics of bite force production and its relationship to diet in bats. Functional Ecology 24:776–784.

Santana, S. E., I. R. Grosse, and E. R. Dumont. 2012. Dietary hardness, loading behavior, and the evolution of skull form in bats. Evolution 66:2587–2598.

Santana, S. E., and S. E. Lofgren. 2013. Does nasal echolocation influence the modularity of the mammal skull? Journal of Evolutionary Biology 26:2520–2526.

Thiagavel, J., C. Cechetto, S. E. Santana, L. Jakobsen, E. J. Warrant, and J. M. Ratcliffe. 2018. Auditory opportunity and visual constraint enabled the evolution of echolocation in bats. Nature Communications 9:98.

Vater, M., and M. Kössl. 2011. Comparative aspects of cochlear functional organization in mammals. Hearing Research 273:89–99.

Veilleux, C. C., and E. C. Kirk. 2014. Visual acuity in mammals: effects of eye size and ecology. Brain, Behavior and Evolution 83:43–53.

Wagner, G. P., M. Pavlicev, and J. M. Cheverud. 2007. The road to modularity. Nature Reviews Genetics 8:921–931.

Warton, D. I., R. A. Duursma, D. S. Falster, and S. Taskinen. 2012. smatr 3—an R package for estimation and inference about allometric lines. Methods in Ecology and Evolution 3:257–259.

Watanabe, A., A. C. Fabre, R. N. Felice, J. A. Maisano, J. Müller, A. Herrel, and A. Goswami. 2019. Ecomorphological diversification in squamates from conserved pattern of cranial integration. Proceedings of the National Academy of Sciences of the USA 116: 14688–14697.

Wiley, D. F., N. Amenta, D. A. Alcantara, D. Ghosh, Y. J. Kil, E. Delson, W. Harcourt-Smith, et al. 2005. Evolutionary morphing. IEEE.

Winter, Y., and O. von Helversen. 2003. Operational tongue length in phyllostomid nectar-feeding bats. Journal of Mammalogy 84:886–896.

Yohe, L. R., M. Fabbri, D. Lee, K. T. Davies, T. P. Yohe, M. K. Sánchez, E. M. Rengifo, et al. 2022. Ecological constraints on highly evolvable olfactory receptor genes and morphology in neotropical bats. Evolution 76:2347–2360.

Zelditch, M. L., and A. Goswami. 2021. What does modularity mean? Evolution and Development 23:377–403.

Associate Editor: Scott J. Steppan
Editor: Daniel I. Bolnick